Superstructures and domain structures in natural and synthetic kalsilite

Huifang Xu* and David R. Veblen

Department of Earth and Planetary Sciences, Johns Hopkins University, Baltimore, Maryland 21218, U.S.A.

Abstract

Transmission electron microscopy (TEM) investigation of natural kalsilite, $(K_{1.77}\square_{0.09}Na_{0.14})_{\Sigma 2}(Si_{2.09}Al_{1.79}Fe_{0.12})_{\Sigma 4}O_8$, from San Venanzo, Italy, shows that it contains a pervasive domain structure related to a superstructure. The probable space group for the superstructure is $P2_1$. The relationship between the unit-cell parameters of the $P6_3$ subcell and those of the $P2_1$ supercell is $a_{super} \cong b_{super} \cong \sqrt{3}a_{sub}$; $c_{super} = c_{sub}$, and the a_{super} axis is rotated 30° about the c axis with respect to the a_{sub} axis. Nonperiodic distribution of elongated twin domains causes streaking of superstructure reflections normal to the c^* axis. The average structure of this kalsilite sample has $P6_3$ symmetry. On the basis of previous structure refinements, this average structure has three O1 positions slightly displaced from the threefold axis, and each O1 position has a site occupancy of ⅓. High-temperature annealing studies indicated that there is a displacive phase transition from the $P2_1$ superstructure to the $P6_3$ substructure. The twin domains are related by threefold twin operations. The phase-transition temperature for kalsilite may range from 500 to 600 °C and is dependent on the crystal composition (e.g., the proportions of Na, Ca, and vacancies).

Kalsilite crystals prepared from nepheline by Na-K exchange are structurally complex. Domain structures in Na-bearing kalsilite crystals with more than 2.5 mol% $NaSiAlO_4$ are similar to those in the natural kalsilite sample but exhibit additional twin boundaries parallel to the c axis. Na-poor and Na-free kalsilite crystals are composed of (0001) domains with $P6_3$ and $P31c$ symmetries, respectively, and merohedral twins between the neighboring $P6_3$ or $P31c$ domains. The merohedral twins in the synthetic crystals formed during transformation of the nepheline structure to the kalsilite structure. The intergrown domains with $P31c$ symmetry formed during the phase transition on cooling of the Na-poor kalsilite. There is no simple symmetry hierarchy among the known structures in the proposed phase diagram.

Introduction

Kalsilite, a mineral found in K_2O-rich and SiO_2-poor volcanic rocks (Bannister and Hey 1942; Bannister and Sahama 1953; Holmes 1942; Sahama 1960), is a stuffed derivative of the tridymite structure (Buerger 1954) with an ordered distribution of Al and Si atoms (Perrotta and Smith 1965; Dollase and Freeborn 1977; Hovis et al. 1992). Recently, nearly pure $KSiAlO_4$ kalsilite was reported from a granulite (Capobianco and Carpenter 1989; Sandiford and Santosh 1991). Kalsilite also forms a crystalline solution with nepheline at high temperatures (Smith and Tuttle 1957; Sahama et al. 1956; Sahama 1960; Ferry and Blencoe 1978; Hovis et al. 1992). The crystal structure of natural kalsilite from the lava of Mount Nyragonga in the eastern Belgian Congo was determined by Perrotta and Smith (1965). Their results indicated that kalsilite has $P6_3$ symmetry with ⅓ occupancy of the apical O atoms at O1 sites (O2 in their notation), which are displaced from the threefold axis (Fig. 1).

However, the crystal used for the structure refinement also showed very weak and diffuse superstructure reflections, indicating a supercell in which $a_{super} = \sqrt{3}a_{sub}$ and a_{super} is rotated 30° about the c axis relative to a_{sub} (Smith and Sahama 1957; Perrotta and Smith 1965). Smith and Sahama (1957) also reported structural variations in kalsilite, noting the disappearance of weak and diffuse superstructure reflections with heating to 600 °C.

Dollase and Freeborn (1977) determined the crystal structure of kalsilite prepared from nepheline by K exchange. Their results showed that the average structure has $P6_3mc$ symmetry, such that the basal O atoms at O2 sites are disordered between two sites related by a mirror. Like Perrotta and Smith (1965), they observed displacement of the O1 site from the threefold axis. Dollase and Freeborn (1977) suggested that twin domains with $P6_3$ symmetry contribute to the apparent positional disorder of the O2 atoms, and that the orientation of the small domains is related by a mirror plane normal to a_{sub}, thereby generating an overall $P6_3mc$ symmetry. High-temperature X-ray diffraction experiments showed a series of phase transitions in hydrothermally synthesized pure kal-
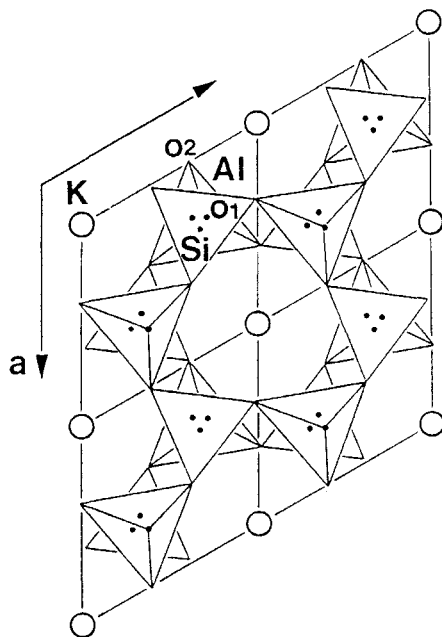
FIGURE 1. Model of the average structure of kalsilite, showing splitting of O1 atoms into three partially occupied sites, each with a site occupancy of ⅓. (Modified from Perrotta and Smith 1965 and Merlino 1984.)

silite. The structure has $P6_3mc$ symmetry above 1138 °C, with hexagonal rather than ditrigonal rings (Andou and Kawahara 1982). There is an unquenchable orthorhombic modulated structure at temperatures above 850 °C and a low-temperature form, probably with $Cmc2_1$ symmetry, below 850 °C (Capobianco and Carpenter 1989; Kawahara et al. 1987). A discontinuity or phase transition at 650 °C was also reported in synthetic crystals (Kawahara et al. 1987). Reinvestigation of a metamorphic kalsilite indicated that the high-temperature modulated phase comprises intergrown hexagonal structures ($6A$, $P6_3mc$ and $1A$, $P6_3$); the low-temperature phase consists of intergrown hexagonal ($1A$, $P6_3mc$) and trigonal ($1A$, $P31c$) kalsilite (Carpenter and Cellai 1996). The $P31c$ structure is the stable form at low temperature, whereas the $P6_3$ structure is stable at high temperature. The phenomena are similar to those in $KLiSO_4$ crystals described by Bansal et al. (1980), Zhang et al. (1988), Rajagopal et al. (1991), and Bhakay-Tamhane et al. (1985, 1991).

In this paper, we describe selected-area electron diffraction (SAED) and transmission electron microscopy

(TEM) studies of natural kalsilite from a melilite porphyry collected from San Venanzo, Italy, and synthetic kalsilite crystals. Observations are reported on superstructures, domain structures, and the real symmetry of the crystals at low temperature. Preliminary results of this paper were presented by Xu and Veblen (1994).

SPECIMENS AND EXPERIMENTAL METHODS

Natural kalsilite crystals for this TEM study are from a specimen from San Venanzo, Italy (USNM 150301). The euhedral, columnar kalsilite crystals in this specimen coexist with euhedral leucite in miarolitic cavities of a melilite porphyry. The crystal selected for study appeared homogeneous with optical microscopy. The porphyritic rock is composed of akermanite, biotite, magnetite, kalsilite, and glassy groundmass. Chemical formulas of kalsilite and related minerals from AEM analyses are listed in Table 1.

Synthetic kalsilite was produced using the method of Dollase and Freeborn (1977) for the Na-K exchange of nepheline. The kalsilite crystals were prepared by mixing KCl and nepheline powder in a 10:1 ratio by weight and annealing at temperatures from 800 to 830 °C for 20 h. The nepheline starting material was from a nepheline syenite in Liaoning Province, northeastern China (Nanjing University Collection). There is no modulation or domain structure in the nepheline, which is characterized by sharp reflections in SAED patterns (Fig. 2). This procedure produced kalsilite crystals in which areas that are thin enough to be transparent to the electron beam are dominated by K (or the kalsilite component, Ks) (Table 2). Both the natural kalsilite and the synthetic kalsilite contain small but measurable amounts of Na, Ca, and excess Si (Tables 1 and 2).

Specimens for TEM experiments were prepared by crushing single kalsilite crystals in an agate mortar and placing a drop of crystal-alcohol suspension on holey carbon-coated copper grids. All TEM and AEM investigations were performed with a Philips 420ST electron microscope equipped with an EDAX energy-dispersive X-ray detector and a Princeton-Gamma Tech analyzer as described by Livi and Veblen (1987). For chemical analyses, Fe was assumed to be Fe^{3+} in kalsilite and Fe^{2+} for the glass groundmass. Chemical formulas of the natural kalsilite and related minerals are listed in Table 1, and formulas of the synthetic materials are given in Table 2. An important experimental obstacle for TEM investigation was extremely fast amorphization damage of the

TABLE 1. Chemical formulas of kalsilite and related minerals

| Mineral	Formula	Note
Kalsilite	$(K_{1.77}\square_{0.09}Na_{0.14})_{\Sigma2.00}[Si_{2.09}Al_{1.79}Fe_{0.12}]_{\Sigma4}O_8$	in miarolitic cavity: Ne = 7
Leucite	$(K_{0.95}Ca_{0.01}Na_{0.04})_{\Sigma1.00}[Si_{1.99}Al_{0.96}Fe_{0.05}]_{\Sigma3}O_6$	in miarolitic cavity
Kalsilite	$(K_{1.70}\square_{0.06}Na_{0.21}Ca_{0.03})_{\Sigma2.00}[Si_{2.03}Al_{1.81}Fe_{0.16}]_{\Sigma4}O_8$	phenocryst: Ne = 12
Akermanite	$(Ca_{1.76}Na_{0.22}Fe_{0.03})_{\Sigma2.01}(Mg_{0.66}Al_{0.19}Fe_{0.15})_{\Sigma1.00}[Si_{1.98}Al_{0.02}]_{\Sigma2}O_7$	phenocryst
Glass	$(K_{0.06}Na_{0.14}Ca_{0.40})_{\Sigma0.60}(Mg_{0.87}Fe_{0.26})_{\Sigma1.15}[Si_{1.95}Al_{0.25}]_{\Sigma2}O_6$	based on pyroxene formula
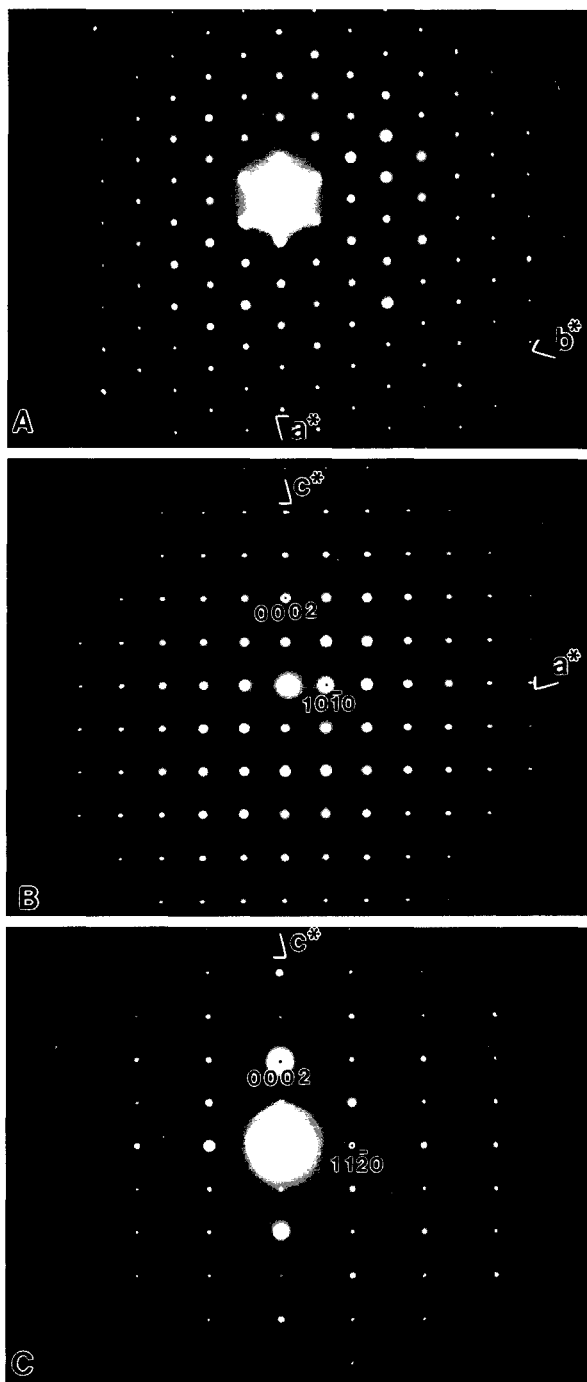
FIGURE 2. SAED patterns of the nepheline used to prepare kalsilite by ion exchange. A–C show three major orientations, all with sharp reflections. The unit-cell parameters of nepheline are doubled along the a and b axes, as a result of an ordered arrangement of K and Na atoms (Dollase and Peacor 1971; Hahn and Buerger 1955).

TABLE 2. Chemical formulas of nepheline and kalsilite from K-exchanged nepheline (determined by AEM)

Mineral	Formula
Nepheline	$(Na_{1.44}K_{0.42}Ca_{0.01}\square_{0.12})_{\Sigma 2.00}[Si_{2.12}Al_{1.87}Fe_{0.01}]_{\Sigma 4}O_8$
Kalsilite	$(K_{1.83}Na_{0.05}Ca_{0.01}\square_{0.11})_{\Sigma 2.00}[Si_{2.11}Al_{1.88}Fe_{0.01}]_{\Sigma 4}O_8$
Kalsilite	$(K_{1.83}Na_{0.05}\square_{0.12})_{\Sigma 2.00}[Si_{2.12}Al_{1.87}Fe_{0.01}]_{\Sigma 4}O_8$
Kalsilite	$(K_{1.82}Na_{0.09}\square_{0.09})_{\Sigma 2.00}[Si_{2.08}Ti_{0.01}Al_{1.90}Fe_{0.01}]_{\Sigma 4}O_8$
Kalsilite*	$(K_{1.92}Na_{0.01}\square_{0.07})_{\Sigma 2.00}[Si_{2.06}Ti_{0.01}Al_{1.92}Fe_{0.01}]_{\Sigma 4}O_8$

* From the crystal used to produce the SAED patterns in Figures 12A and 12B.

specimens in the electron beam, thereby limiting our ability to obtain high-resolution TEM (HRTEM) images.

TEM RESULTS AND DISCUSSION

Natural kalsilite

Selected-area electron diffraction patterns. A [0001] zone-axis SAED pattern of the natural kalsilite sample (Fig. 3A) shows weak and diffuse superstructure reflections between the sharp main Bragg reflections characteristic of the $P6_3$ kalsilite subcell. The superstructure reflections indicate a supercell with $a_{super} \cong b_{super} \cong \sqrt{3}a_{sub}$ and a rotation of the a_{super} axis by 30° about the c axis with respect to the a_{sub} axis. The SAED pattern in Figure 3A shows hexagonal or pseudohexagonal symmetry of the superstructure. A c^*-$[01\bar{1}0]^*$ SAED pattern (Fig. 3B) shows sharp main reflections characteristic of the $P6_3$ subcell, with weak superstructure reflections indicating tripled periodicity along the $[01\bar{1}0]^*$ direction. The intensities of the l = odd reflections are weaker than those of the l = even reflections (Fig. 3B). The superstructure reflections are also weakly streaked normal to the c^* axis, suggesting that there is a domain structure in the crystal composed of elongated domains parallel to the c axis. However, SAED patterns of the c^*-$[11\bar{2}0]^*$ plane (Fig. 2C) do not show superstructure reflections or diffuse streaking, as is expected from Figure 3A. The SAED pattern in Figure 3D shows extinction of the $00l$ (l = odd) diffraction spots and weak superstructure reflections along $[12\bar{3}0]^*$.

TEM images. All dark-field (DF) images formed from single, diffuse superstructure reflections of the natural kalsilite sample reveal a pervasive domain structure. The DF image in Figure 4A, which corresponds to the orientation of the SAED pattern in Figure 3A, shows equidimensional domains in the (0001) plane. However, DF images corresponding to the orientations in Figures 3B and 3D show elongated domains parallel to the c axis (Figs. 4B and 4C, respectively). The projected dimensions of the elongated domains are about 10 × 30 nm. An HRTEM image (Fig. 5) corresponding to the orientation of the SAED pattern in Figure 3B shows $(01\bar{1}0)_{super}$ superlattice fringes with a periodicity of 7.8 Å, and elongated contrast anomalies along the c axis as a result of small domains. The neighboring domains in kalsilite revealed by DF and HRTEM images (Figs. 4 and 5) are probably related to each other by twinning operations.
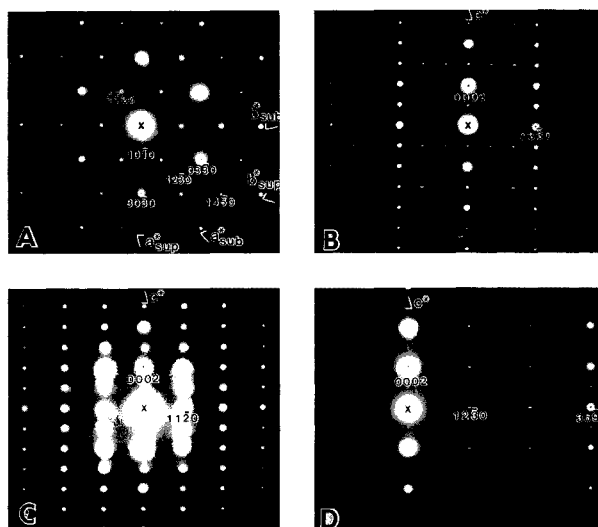
FIGURE 3. SAED patterns of kalsilite from a melilite porphyry of San Venanzo, Italy. Indexing of the diffraction patterns is based on the hexagonal supercell setting (see text). (A) The [0001] zone-axis SAED pattern showing weak, diffuse superstructure reflections and strong main Bragg reflections. (B) SAED pattern showing the c^*-[01$\bar{1}$0]* plane with weak, streaked superstructure reflections indicating tripled superstructure periodicity in the [01$\bar{1}$0]* direction. (C) SAED pattern showing the c^*-[11$\bar{2}$0]* plane with sharp main Bragg reflections only. (D) SAED pattern showing the c^*-(12$\bar{3}$0)* plane with weak and streaked superstructure reflections.

High-temperature annealing. Natural kalsilite crystals were annealed in air at 1 atm and temperatures of 800 and 900 °C. After the crystals were annealed for 10 min, they were quenched to room temperature in air. Crystals annealed at 800 °C show very weak, diffuse superstructure reflections in [0001]-zone SAED patterns (Fig. 6A). Crystals annealed at 900 °C show no superstructure reflections in [0001]-zone SAED patterns (Fig. 6B), but there is extremely weak and continuous streaking in the positions previously occupied by superstructure reflections in the c^*-[01$\bar{1}$0]* SAED pattern (Fig. 6C).

These annealing experiments indicate that kalsilite loses its superstructure at high temperature, probably transforming into a high-symmetry phase with space group $P6_3$. On the basis of the structural differences observed in X-ray diffraction studies between the superstructure and hexagonal substructure (Perrotta and Smith 1965; Kawahara et al. 1987), this phase transition probably involves positional disordering of O1 atoms and framework distortion. The weak streaking in the annealed kalsilite may be caused by very small superstructure domains. The average structure of kalsilite characterized by extremely weak and continuous reflections in the positions of superstructure reflections (Figs. 6B and 6C) is hexagonal, with space group $P6_3$, and corresponds to the idealized kalsilite structure determined by Smith and Sahama (1957). The relatively fast transition from superstructure
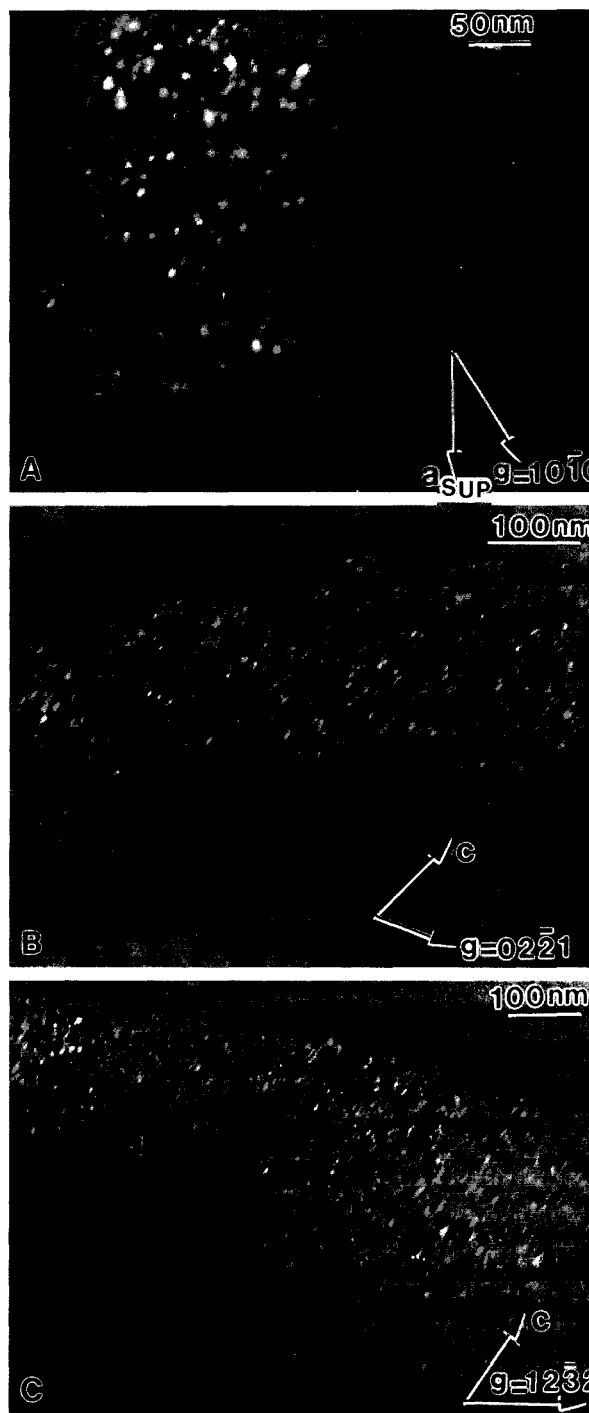

FIGURE 4. (A) Dark-field (DF) image ($g = 10\bar{1}0$) of natural kalsilite corresponding to the orientation of the SAED pattern in Figure 3A, showing equidimensional domains on the (0001) plane. (B) DF image ($g = 02\bar{2}1$) of natural kalsilite corresponding to the orientation of the SAED pattern in Figure 3B, showing domains elongated parallel to the c axis. (C) DF image ($g = 12\bar{3}2$) of natural kalsilite corresponding to the orientation of the SAED pattern in Figure 3D, showing domains elongated parallel to the c axis.
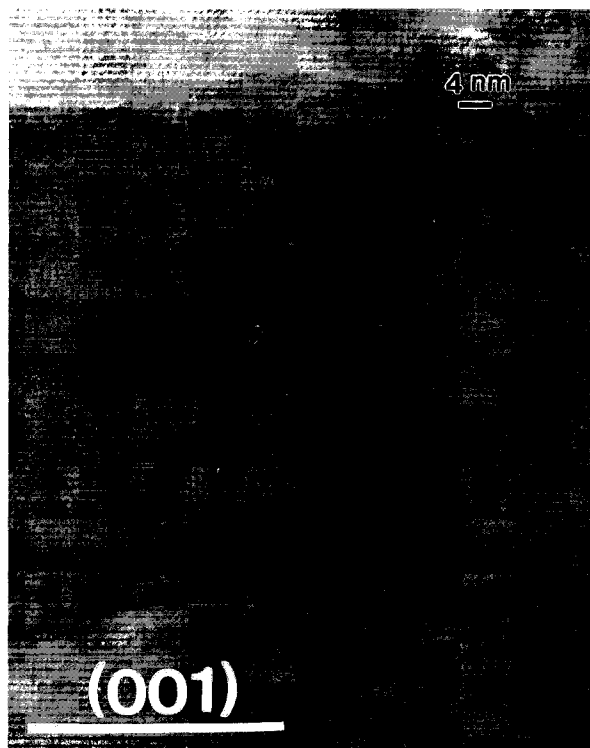
FIGURE 5. HRTEM image of natural kalsilite corresponding to the orientation of the SAED pattern in Figure 3B and the DF image in Figure 4B, showing elongated domains characterized by anomalies in contrast. (Best seen by viewing at a low angle.)

to substructure indicates that the mechanism of the phase transition is probably displacive or displacive-like, on the basis of Buerger's classification for phase transitions (Buerger 1972). The intensity of the streaked superstructure reflections is inversely proportional to the domain size in the crystal and is also related to the displacement magnitude of the O1 atoms off the threefold axis positions. It is possible that, with sufficiently fast cooling, ideal hexagonal kalsilite with $P6_3$ symmetry could be quenched to room temperature.

Discussion of the superstructure and the domain structure and their formation. The superstructure reflections in SAED patterns (Figs. 3A and 3B) indicate a supercell with $a_{super} \cong b_{super} \cong \sqrt{3}a_{sub}$ and a rotation of the a_{super} axis by 30° about the c axis. The symmetry of the kalsilite may be hexagonal or pseudohexagonal (e.g., orthorhombic or monoclinic). The relationship between the unit-cell parameters of the hexagonal supercell and those of the hexagonal subcell is $a_{super} = b_{super} = \sqrt{3}a$; $c_{super} = c_{sub}$. However, the superstructure alternatively could have monoclinic symmetry, $P2_1$, one of the subgroups of $P6_3$, and the monoclinic unit-cell parameters (hexagonal setting) would be $a_{super} \cong b_{super} \cong \sqrt{3}a_{sub}$; $\alpha \cong 120°$; $\beta \cong \gamma \cong 90°$.

A possible structure for kalsilite at room temperature is shown in Figure 7. In this superstructure model, the
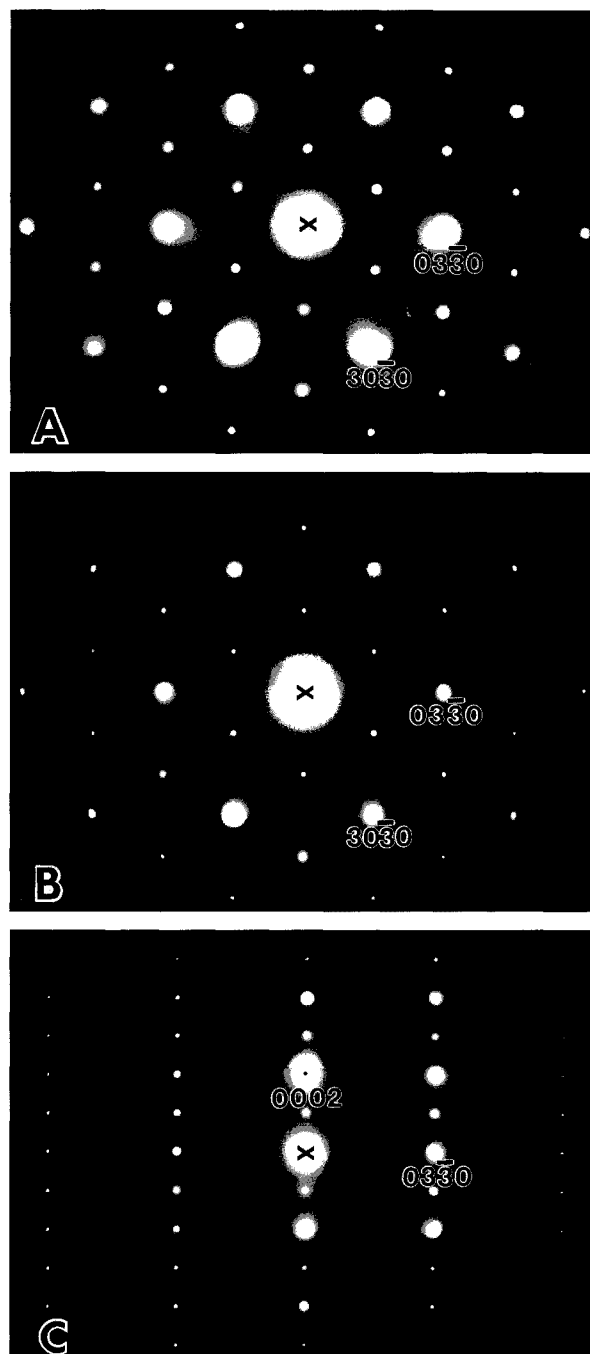

FIGURE 6. (A) The [0001] zone-axis SAED pattern of kalsilite annealed at 800 °C, showing very weak and diffuse superstructure reflections. (B) The [0001] zone-axis SAED pattern of kalsilite annealed at 900 °C, showing no superstructure reflections. (C) SAED pattern showing the c^*-[01$\bar{1}$0]* plane of kalsilite annealed at 900 °C, with continuous and extremely weak reflections in the positions of the superstructure reflections. Indexing of all reflections is based on the hexagonal supercell setting, as in Figure 3.
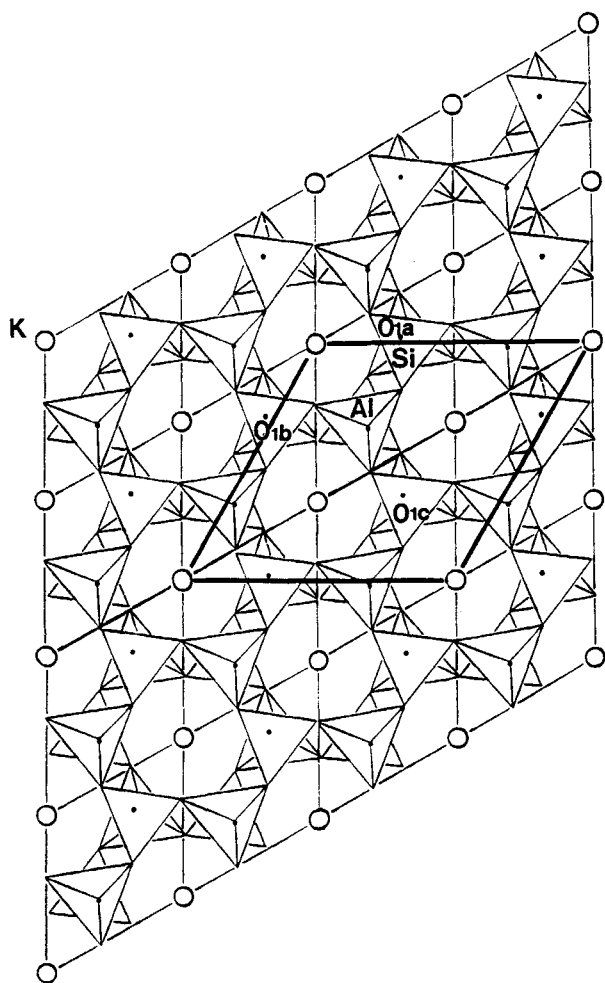
FIGURE 8. Structural model of kalsilite with twin-domain structure, showing three $P2_1$ superstructure domains related by a threefold twinning operation. Arrows indicate twin-domain boundaries. Supercells in each domain are indicated by heavy lines.

FIGURE 7. Schematic model of the superstructure in kalsilite with space group $P2_1$, showing displacement of O1 atoms off the threefold-axis positions (O1a, O1b, O1c). Hexagonal subcells are outlined by light lines, and one supercell is outlined by heavy lines.

O1 atoms of the $P6_3$ structure shown in Figure 1 are displaced into fully occupied O1a, O1b, and O1c sites. This monoclinic superstructure is metrically hexagonal and would display pseudohexagonal symmetry. If the superstructure of kalsilite had $P6_3$ symmetry, rather than $P2_1$, the O1a, O1b, and O1c atoms would be symmetrically identical, and the supercell would not exist, which is not consistent with the observed superstructure reflections. Thus, if this superstructure is correct, $P2_1$ is the likely symmetry, rather than $P6_3$.

The phenomena of domain structure and average structure in kalsilite are similar to those in low-symmetry vesuvianite with a twin-domain structure. The true symmetry of vesuvianite domains (possibly $P2_1/n$) is lower than that of the disordered high-temperature structure ($P4/nnc$) (Veblen and Wiechmann 1991), but the average structure of vesuvianite may display tetragonal symmetry
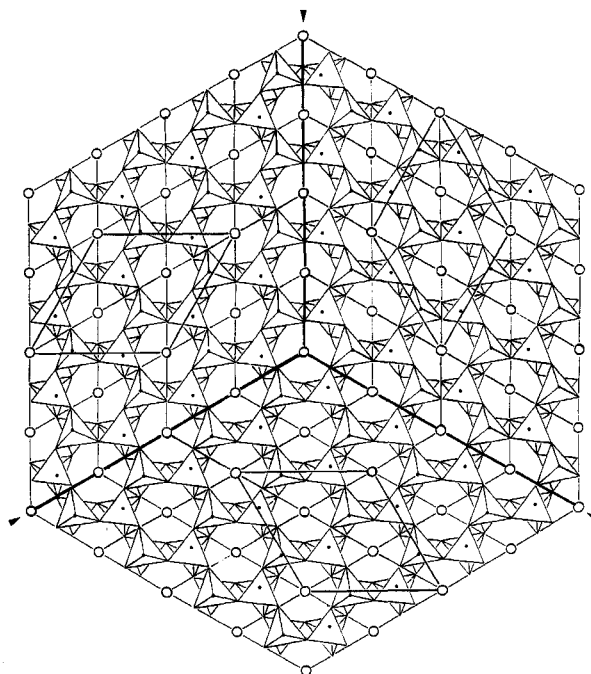
with space group $P4/nnc$. Each domain in vesuvianite is also metrically tetragonal within experimental error.

Euhedral leucite crystals coexisting with the natural kalsilite contain both merohedral and pseudomerohedral twin structures that probably formed during the phase transition from cubic ($Ia3d$) to tetragonal ($I4_1/a$) symmetry, as suggested by the in situ heating experiments of Heaney and Veblen (1990). The temperature of the phase transition of leucite from cubic to tetragonal symmetry is about 650 °C (Heaney and Veblen 1990). The crystallization temperatures of the kalsilite and its coexisting euhedral leucite should be the same and higher than the phase-transition temperature (~650 °C) of leucite.

We suggest that Na-bearing natural kalsilite that has crystallized at temperatures above 650 °C has $P6_3$ symmetry. As the kalsilite crystals cool, they pass through the phase-transition temperature, which may range from 500 to 600 °C and depends on the composition of kalsilite. On the basis of the relationships between domain boundaries and space groups for cell-preserved phase transitions (Van Tendeloo and Amelinckx 1974; Guymont 1978; Xu et al. 1993), it can be inferred that the phase transition from the $P6_3$ substructure to the $P2_1$ superstructure results in antiphase domains and twin domains involving threefold rotation. The series of DF images formed with streaked superstructure reflections (Fig. 4) shows small, elongated domains consistent with such boundaries, but, as a result of the small domain size and
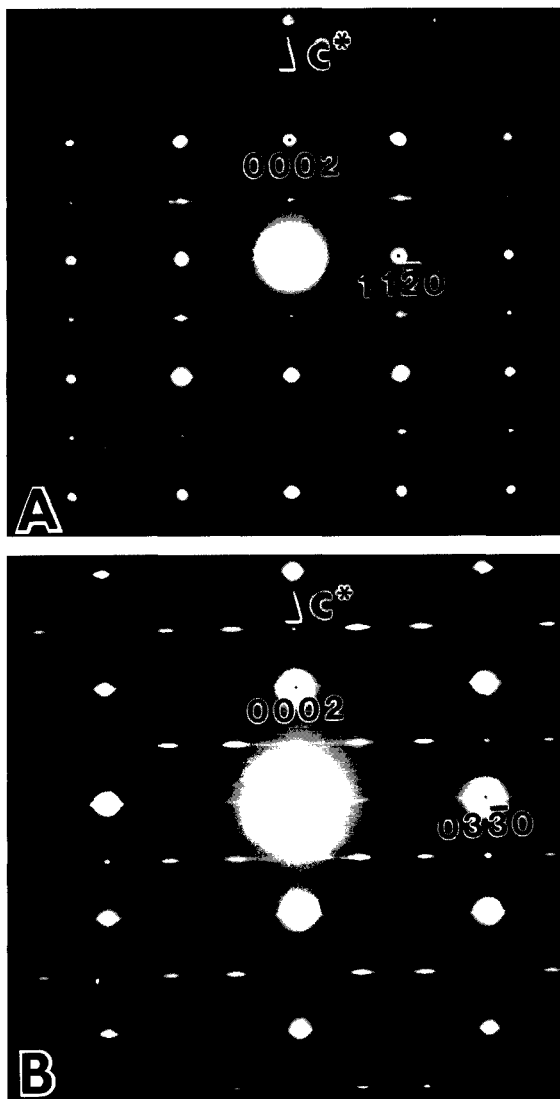
Figure 9. SAED patterns of a synthetic kalsilite grain, showing reflections in the c^*-$[11\bar{2}0]^*$ plane (A) and the c^*-$[01\bar{1}0]^*$ plane (B). Indexing is based on the hexagonal setting of the substructure unit cell, even though the superstructure is apparently monoclinic.
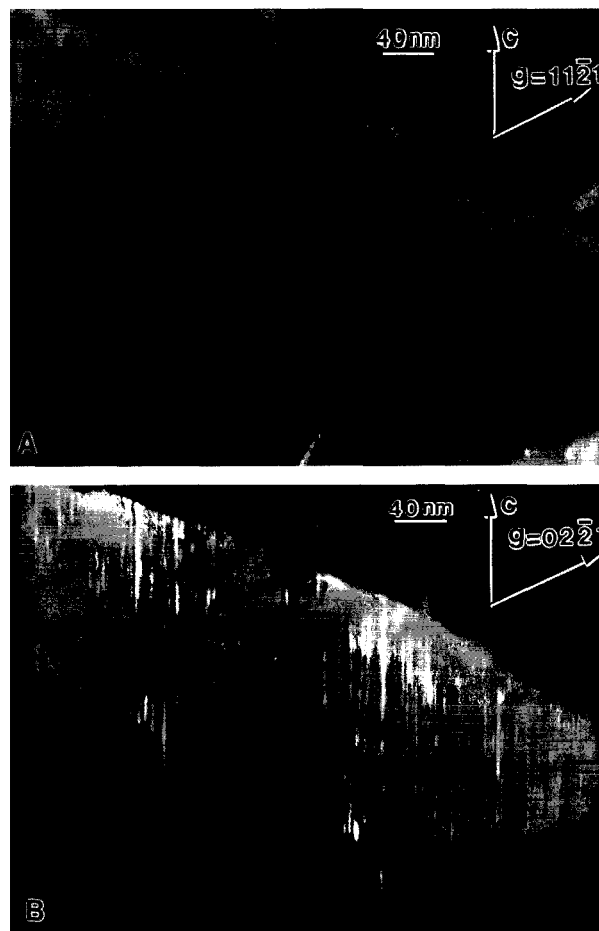

Figure 10. DF images of synthetic kalsilite formed by using one reflection from SAED patterns in Figure 9A (A; $g = 11\bar{2}1$) and Figure 9B (B; $g = 02\bar{2}1$).

fast radiation damage, it was impossible to identify antiphase and twin domains more rigorously. The possible translations between neighboring antiphase domains, if any exist, are ($a_{super}/3 + 2b_{super}/3$) and ($2a_{super}/3 + b_{super}/3$). Figure 8 illustrates $P2_1$ superstructure domains that are twin related by the threefold-rotation axis that is lost at the phase transition from $P6_3$ to $P2_1$ symmetry. The twin boundaries do not have to be straight in the real crystal. In each domain, a supercell with $P2_1$ symmetry is illustrated by heavy lines. The average structure of kalsilite composed of twin domains of this sort displays $P6_3$ symmetry with site occupancies of ⅓ for O1 atoms off the threefold axis positions, as reported by Perrotta and Smith

(1965). The streaking of superstructure reflections normal to the c^* axis observed in SAED patterns may be caused by nonperiodic arrangement of elongated superstructure domains of this sort.

Synthetic kalsilite

Na-bearing kalsilite. TEM observations show that the K-exchanged crystals are heterogeneous in structure and differ from grain to grain. Figure 9 shows SAED patterns in two orientations of a synthetic kalsilite grain. The indexing of all SAED patterns of the kalsilite with more than 2.5 mol% $NaSiAlO_4$ is based on the $P2_1$ superstructure and hexagonal unit-cell setting because they display superstructure reflections similar to those of the natural kalsilite. The c^*-$[11\bar{2}0]^*$ reciprocal lattice plane (Fig. 9A) shows relatively streaked and weak l = odd reflections. The intensities of the streaking and the diffraction maxima differ from grain to grain. The c^*-$[01\bar{1}0]^*$ SAED pattern (Fig. 9B) is similar to that from the natural kalsilite sample, except that no superstructure reflections appear in the l = even rows. Streaking of the superstructure
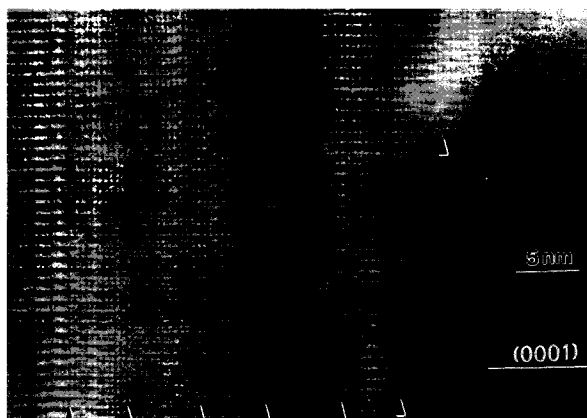
FIGURE 11. HRTEM image of synthetic kalsilite corresponding to the orientation in Figures 9A and 10A, showing possible twin boundaries parallel to the c axis.

reflections is consistent with superstructure domains similar to those in the natural kalsilite sample. AEM analyses showed that the grains that yield intensely streaked diffraction patterns are relatively rich in Na (Table 2).

DF images formed with the $11\bar{2}1$ reflection show a very thin domain parallel to the c axis (Fig. 10A), as do images formed with the $02\bar{2}1$ reflection (Fig. 10B). The superstructure domains imaged by the streaked $02\bar{2}1$ reflection are similar to those in the natural kalsilite. The domains in Figure 10A are wider than the superstructure domains in Figure 10B. An HRTEM image corresponding to the orientation in Figure 10A also shows probable domain boundaries parallel to the c axis, as indicated by arrows (Fig. 11). The neighboring domains with $P2_1$ symmetry in the HRTEM image are related by mirror planes parallel to the c axis, which are similar to the twin boundaries proposed by Dollase and Freeborn (1977), and they are not observed in the natural kalsilite sample. It is likely that the ditrigonal rings in the neighboring kalsilite domains in Figures 10 and 11 are in opposite orientations, which were produced during transformation of the neutral nepheline structure to the kalsilite structure.

Na-poor kalsilite. The chemical composition of the crystal is richer in K than the grains that produced the SAED patterns shown in Figure 9 (Table 2). SAED patterns of Na-poor kalsilite grains show weak streaking along c^* and very weak streaking normal to c^* (Figs. 12A and 12B). Indexing of the diffraction patterns of this kalsilite grain is based on the hexagonal subcell setting of normal $P6_3$ kalsilite because there are no obvious superstructure reflections. Very weakly streaked reflections normal to c^* are caused by elongated twin domains parallel to the c axis, which also occur in the Na-bearing kalsilite (Figs. 9A, 10A, and 11). These twin domains possibly reflect the splitting of O2 atoms over two sites, as described by Dollase and Freeborn (1977). Reflections streaked along c^* were also reported in a kalsilite sample described by Dollase and Freeborn (1977). A DF image
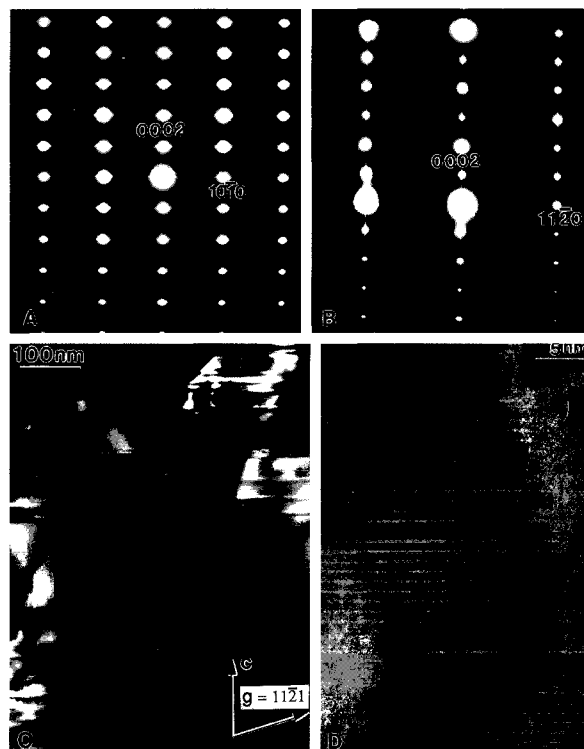

FIGURE 12. Synthetic kalsilite. (**A**) SAED pattern showing the c^*-$[10\bar{1}0]^*$ plane. (**B**) SAED pattern showing the c^*-$[11\bar{2}0]^*$ plane. (**C**) DF image, $g = 11\bar{2}1$. (**D**) HRTEM image showing domains and boundaries with 8.7 and 4.35 Å periodicities, respectively.

(Fig. 12C; $g = 11\bar{2}1$) shows domains and wide boundaries between the domains parallel to (0001), as also observed in a natural Na-free kalsilite (Capobianco and Carpenter 1989; Carpenter and Cellai 1996). A one-dimensional lattice image corresponding to the orientation in Figures 12B and 12C shows domains with 8.7 Å periodicity, separated by boundaries with 4.35 Å periodicity (Fig. 12D). The domain structure in this crystal grain is similar to that in Na-free kalsilite from a granulite described by Capobianco and Carpenter (1989) and Carpenter and Cellai (1996). According to the results of Carpenter and Cellai (1996), we propose that the SAED pattern in Figure 12B is an overlapped diffraction pattern from both $P6_3$ and $P31c$ domains. Domains with 8.7 Å periodicity and boundaries with 4.35 Å periodicity are the intergrown domains with $P6_3$ and $P31c$ symmetries, respectively. Figure 13 illustrates the relationships among $P31c$ and $P6_3$ domains and their merohedral twins. The boundary between two neighboring $P6_3$ merohedral twin domains is a unit of $P31c$ structure; the boundary between two neighboring $P31c$ merohedral twin domains is a unit of $P6_3$ structure (Figs. 12D and 13). The merohedral twins are similar to those in the $KLiSO_4$ crystal studied by Schulz et al. (1985), Zhang et al. (1988), Chen and Wu (1989), and BhakayTamhane et al. (1984, 1985,

role of nuclei of $P31c$ structure during the transition from $P6_3$ to $P31c$ symmetry. The existence of these extended twin boundaries may reduce the nucleation-energy barrier of the phase transition between $P6_3$ and $P31c$ structures.

The average structure of a crystal with such a domain structure may be complex, e.g., degenerate O-atom positions (O1 and O2), if structure refinement is based on the $P6_3mc$ substructure. The merohedral twins between $P6_3$ domains probably formed during transformation of the neutral nepheline structure to the kalsilite structure at about 800 °C during the Na-K–exchange experiment. The intergrown $P31c$ domains were formed by the phase transition from $P6_3$ to $P31c$ structure during cooling of the sample.

SUBSOLIDUS PHASE RELATIONS ON THE KALSILITE-RICH SIDE OF THE NEPHELINE-KALSILITE SYSTEM

Both natural and synthetic low-temperature kalsilite crystals apparently can have either $P2_1$ or $P31c$ symmetry in Na-bearing and Na-poor kalsilite, respectively. The Na-bearing kalsilite sample (Table 1) from an alkali volcanic rock has a superstructure with probable $P2_1$ symmetry. Kalsilite specimens with similar superstructure reflections reported by Smith and Sahama (1957) and Perrotta and Smith (1965) were also from volcanic rocks. Those samples also may have contained a substantial nepheline component, but no compositional information is available. Synthetic, Na-bearing kalsilite crystals prepared by K-Na exchange of nepheline (Table 2) display superstructure reflections in SAED patterns (Fig. 9) that are similar to those in the natural Na-bearing kalsilite. In contrast, reported natural and synthetic kalsilite with intergrown $P6_3$ and $P31c$ domains is almost Na free. Similarly, the (0001) domains in the Na-poor kalsilite prepared by Dollase and Freeborn (1977) also apparently have complex twinning. The very K-rich regions of the present synthetic kalsilite, which was also prepared by K exchange of nepheline, are composed of similar intergrown $P6_3$ and $P31c$ domains and merohedral twins.

These observations suggest that at low temperatures there may be a phase boundary between the $P2_1$ superstructure and the $P31c$ structure near the kalsilite side of the nepheline-kalsilite phase diagram (Fig. 14). The main difference between the $P2_1$ and $P31c$ structures is the successive (0001) layers of ditrigonal rings having a staggered conformation in the former structure in comparison with the eclipsed conformation in the latter. There is another phase boundary in Na-bearing kalsilite between the $P2_1$ and $P6_3$ structures at about ~500–600 °C. The phase-transition temperature increases as the content of Na in the crystal increases (Fig. 14), a behavior similar to that of the displacive phase transition in Na-rich alkali feldspar (Kroll and Bambauer 1971; Kroll et al. 1980; Xu et al. 1995). Na content and order-disorder of Na and K atoms may play an important role in the phase transition. In Figure 14A the equilibrium phase relations are shown on the kalsilite side of the diagram, whereas Figure 14B
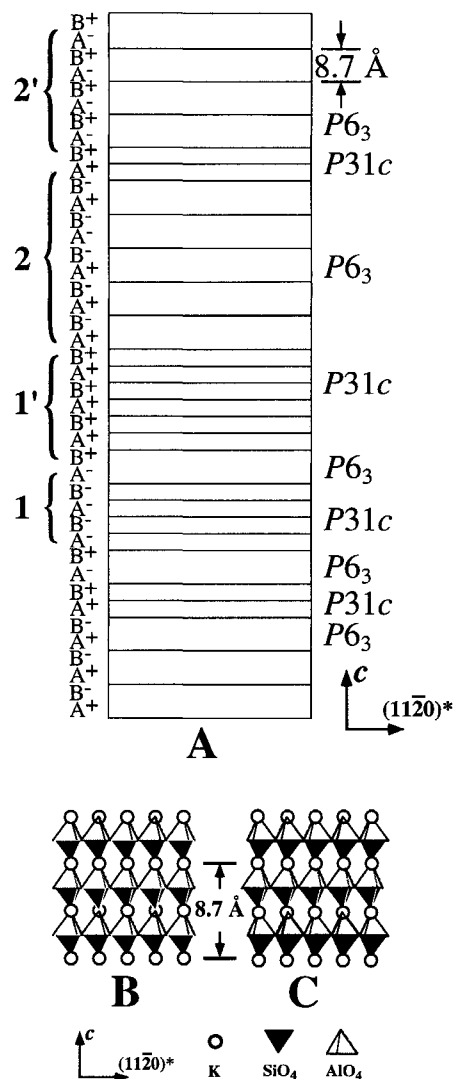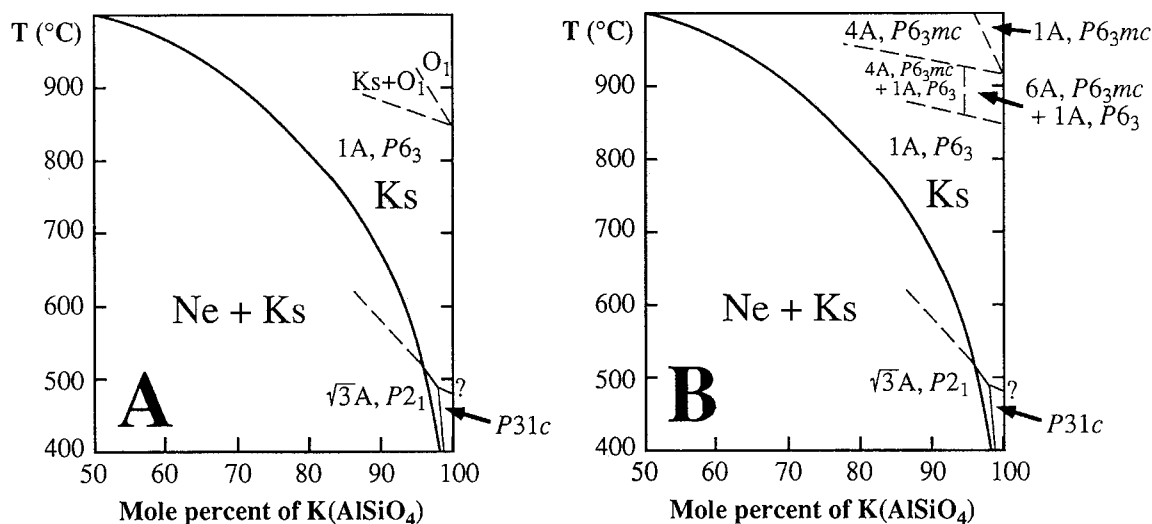

FIGURE 13. (A) Diagram showing stacking of layer domains with $P6_3$ and $P31c$ symmetries in the HRTEM image in Figure 12D. The domains labeled 1 and 1' are merohedral twins with $P31c$ symmetry. The domains labeled 2 and 2' are merohedral twins with $P6_3$ symmetry. A$^+$, A$^-$, B$^+$, and B$^-$ represent (0001) tetrahedral layers with different conformations in the kalsilite. The structures with $P31c$ and $P6_3$ symmetries projected down [2$\bar{1}$0] are illustrated in B and C, respectively.

1991). Such twin boundaries may be called extended twin boundaries. Similar domain boundaries occur in the $KNbW_2O_9$ crystal (Tao et al. 1988). Labels for the stacking sequences of the (0001) tetrahedral layers on the left side of Figure 13 follow the notation proposed by Carpenter and Cellai (1996). The boundaries may play an important role in the $P6_3$-to-$P31c$ transition. The extended twin boundaries between the neighboring $P31c$ domains play the role of nuclei of $P6_3$ structure during the transition from $P31c$ to $P6_3$ symmetry; the extended twin boundaries between the neighboring $P6_3$ domains play the

FIGURE 14. Suggested phase diagrams for the kalsilite-rich side of the nepheline-kalsilite system, showing a series of kalsilite structures. Diagram **A** represents the system at thermodynamic equilibrium. Diagram **B** is a metastable phase diagram for the system without changes in the SiAlO$_4$ framework (i.e., only displacive transitions allowed). The high-temperature phase boundaries in **A** are from Tuttle and Smith (1958). The high-temperature phase boundaries in **B** are from Carpenter and Cellai (1996). The solvus is for 2 kbar (from Ferry and Blencoe 1978).

shows the metastable relations for heating and cooling of kalsilite crystals without reorganization of the tetrahedral framework, which occurs in the transition between kalsilite and kaliophilite. All the transformations in this system appear to be displacive-like, except for those between kaliophilite (O1) and kalsilite (1A, $P6_3$) plus kaliophilite (Ks + O1), and between $P6_3$ kalsilite (Ks-$P6_3$) and kalsilite (1A, $P6_3$) plus kaliophilite (Ks + O1). The phase transformation between kalsilite and kaliophilite changes the structural topology by breaking first-coordination bonds (Smith and Tuttle 1957) and hence is not displacive.

The suggested phase diagrams in Figure 14 show that (K,Na)AlSiO$_4$ crystallizes in the kaliophilite structure at high temperature, rather than high kalsilite with $P6_3mc$ symmetry, because there is no stability field for high kalsilite. Kaliophilite is the stable high-temperature polymorph. Lower temperature forms are $P6_3$ kalsilite and low kalsilite with a superstructure for Na-bearing crystals, and $P31c$ kalsilite for crystals that are almost Na-free. It is suggested that merohedral twin domains in natural kalsilite probably formed during crystallization, rather than during a phase transition from high-temperature kalsilite, on the basis of the phase diagrams.

ACKNOWLEDGMENTS

REFERENCES CITED

Andou, Y., and Kawahara, A. (1982) The existence of high-low inversion point in kalsilite. Mineralogical Journal, 11, 72–77.

Bannister, F.A., and Hey, M.H. (1942) Kalsilite, a polymorph of KAlSiO$_4$ from Uganda. Mineralogical Magazine, 26, 218–224.

Bannister, F.A., and Sahama, Th.G. (1953) Kalsilite in venanzite from San Venanzo, Umbria, Italy. Mineralogical Magazine, 30, 46–48.

Bansal, M.L., Deb, S.K., Roy, A.P., and Sahni, V.C. (1980) New phase transition in LiKSO$_4$. Solid State Communications, 36, 1047–1050.

Bhakay-Tamhane, S., Sequeira, A., and Chidambara, R. (1984) Structure of lithium potassium sulphate, LiKSO$_4$: A neutron diffraction study. Acta Crystallographica, C40, 1648–1651.

———(1985) Low-temperature phase transitions in LiKSO$_4$: A neutron diffraction study. Solid State Communications, 53, 197–200.

———(1991) Phase transitions in LiKSO$_4$: Low-temperature neutron diffraction results. Phase Transitions, 35, 75–98.

Buerger, M.J. (1954) The stuffed derivatives of the silica structures. American Mineralogist, 39, 600–614.

———(1972) Phase transformations. Soviet Physics—Crystallography, 16, 959–968.

Capobianco, C., and Carpenter, M. (1989) Thermally induced changes in kalsilite (KAlSiO$_4$). American Mineralogist, 74, 797–811.

Carpenter, M.A., and Cellai, D. (1996) Microstructures and high-temperature phase transitions in kalsilite. American Mineralogist, 81, 561–584.

Chen, R.H., and Wu, R.T. (1989) An X-ray diffraction study of structural phase transitions of lithium potassium sulphate. Journal of Physics: Condensed Matter, 1, 6913–6920.

Dollase, W.A., and Peacor, D.R. (1971) Si-Al ordering in nepheline. Contributions to Mineralogy and Petrology, 30, 129–134.

Dollase, W.A., and Freeborn, W.P. (1977) The structure of KAlSiO$_4$ with $P6_3mc$ symmetry. American Mineralogist, 62, 336–340.

Ferry, J.M., and Blencoe, J.G. (1978) Subsolidus phase relations in the nepheline-kalsilite system at 0.5, 2.0, and 5.0 kbar. American Mineralogist, 63, 1225–1240.

Guymont, M. (1978) Domain structure arising from transitions between two crystals whose space groups are group-subgroup related. Physical Review B, 18, 5385–5393.

Hahn, T., and Buerger, M.J. (1955) The detailed structure of nepheline, KNa$_3$Al$_4$Si$_4$O$_{16}$. Zeitschrift für Kristallographie, 106, 303–338.

Heaney, P.J., and Veblen, D.R. (1990) A high-temperature study of the low-high leucite phase transition using the transmission electron microscope. American Mineralogist, 75, 464–476.

Holmes, A. (1942) A suite of volcanic rocks from south-west Uganda containing kalsilite (a polymorph of $KAlSiO_4$). Mineralogical Magazine, 26, 197–217.

Hovis, G.L., Spearing, D.R., Stebbins, J.F., Roux, J., and Clare, A. (1992) X-ray powder diffraction and ^{23}Na, ^{27}Al, and ^{29}Si MAS-NMR investigation of nepheline-kalsilite crystalline solutions. American Mineralogist, 77, 19–29.

Kawahara, A., Andou, Y., Marumo, F., and Okuno, M. (1987) The crystal structure of high temperature form of kalsilite ($KAlSiO_4$) at 950 °C. Mineralogical Journal, 13, 260–270.

Kroll, H., and Bambauer, H.-U. (1971) The displacive transformation of (K,Na,Ca)-feldspars. Neues Jahrbuch für Mineralogie Monatshefte, 413–416.

Kroll, H., Bambauer, H.-U., and Schirmer, U. (1980) The high albite–monalbite and analbite-monalbite transitions. American Mineralogist, 65, 1192–1211.

Livi, K.J.T., and Veblen, D.R. (1987) "Eastonite" from Easton, Pennsylvania: A mixture of phlogopite and a new form of serpentine. American Mineralogist, 72, 113–125.

Merlino, S. (1984) Feldspathoids: Their average and real structures. In W.L. Brown, Ed., Feldspars and feldspathoids, p. 435–472. Reidel, Dordrecht, the Netherlands.

Perrotta, A.J., and Smith, J.V. (1965) The crystal structure of kalsilite, $KAlSiO_4$. Mineralogical Magazine, 35, 588–595.

Rajagopal, H., Jaya, V., Sequeira, A., and Chidambaram, R. (1991) Neutron profile refinement study of the low-temperature structural phases of $LiKSO_4$. Physica, B174, 95–100.

Sahama, Th.G. (1960) Kalsilite in the lavas of Mt. Nyiragongo (Belgian Congo). Journal of Petrology, 1, 146–171.

Sahama, Th.G., Neuvonen, K.J., and Hytonen, K. (1956) Determination of the composition of kalsilites by an X-ray method. Mineralogical Magazine, 31, 200–208.

Sandiford, M., and Santosh, M. (1991) A granulite facies kalsilite-leucite-hibonite association from Punalar, Southern India. Mineralogy and Petrology, 43, 225–236.

Schulz, H., Zucker, U., and Frech, R. (1985) Crystal structure of $KLiSO_4$ as a function of temperature. Acta Crystallographica, B41, 21–26.

Smith, J.V., and Sahama, Th.G. (1957) Order-disorder in kalsilite. American Mineralogist, 42, 287–288.

Smith, J.V., and Tuttle, O.F. (1957) The nepheline-kalsilite system: I. X-ray data for the crystalline phases. American Journal of Science, 255, 282–305.

Tao, Y., Hu, M., and Feng, D. (1988) Direct observation of α-β phase transition in $KNbW_2O_9$ by transmission electron microscopy. Physica Status Solidi, A109, 435–444.

Tuttle, O.F., and Smith, J.V. (1958) The nepheline-kalsilite system: II. Phase relations. American Journal of Science, 256, 571–589.

Van Tendeloo, G., and Amelinckx, S. (1974) Group-theoretical considerations concerning domain formation in ordered alloys. Acta Crystallographica, A30, 431–439.

Veblen, D.R., and Wiechmann, M.J. (1991) Domain structure of low-symmetry vesuvianite from Crestmore, California. American Mineralogist, 76, 397–404.

Xu, H., Xu, H., and Luo, G. (1993) A group-theoretical study on the space group of ordered omphacite. Acta Mineralogica Sinica, 13, 1–6.

Xu, H., and Veblen, D.R. (1994) Superstructures and domain structures in kalsilite ($KAlSiO_4$): A framework silicate with derivative structure of tridymite. Abstracts with Programs of the GSA Annual Meeting, 26, A-112.

Xu, H., Veblen, D.R., and Zhang, Y. (1995) Structural modulation and phase transition in a Na-rich alkali feldspar. American Mineralogist, 80, 897–906.

Zhang, P.L., Yan, Q.W., and Boucherle, J.X. (1988) Crystal structure of $KLiSO_4$ at 200 K: A neutron diffraction study. Acta Crystallographica, C44, 592–595.